Biochimie 107 (2014) 270–276

Contents lists available at ScienceDirect

Biochimie

journal homepage: www.elsevier.com/locate/biochi

Research paper

Insights in the kinetic mechanism of the eukaryotic Baeyer–Villiger monooxygenase $BVMO_{Af1}$ from *Aspergillus fumigatus* Af293

María Laura Mascotti [a, *], Marcela Kurina-Sanz [a], Maximiliano Juri Ayub [b], Marco W. Fraaije [c]

[a] INTEQUI-CONICET, Facultad de Química Bioquímica y Farmacia, Universidad Nacional de San Luis, CP 5700 San Luis, Argentina
[b] IMIBIO-SL CONICET, Facultad de Química Bioquímica y Farmacia, Universidad Nacional de San Luis, CP 5700 San Luis, Argentina
[c] Molecular Enzymology Group, Groningen Biomolecular Sciences and Biotechnology Institute, University of Groningen, Nijenborgh 4, 9747 AG Groningen, The Netherlands

ARTICLE INFO

Article history:
Received 28 May 2014
Accepted 5 September 2014
Available online 16 September 2014

Keywords:
Baeyer–Villiger monooxygenases
$BVMO_{Af1}$
Aspergillus fumigatus
Kinetic mechanism
Site-directed mutagenesis

ABSTRACT

This work reports a detailed kinetic study of the recently discovered $BVMO_{Af1}$ from *Aspergillus fumigatus* Af293. By performing steady state and pre-steady state kinetic analyses, it was demonstrated that the rate of catalysis is partially limited by the NADPH-mediated reduction of the flavin cofactor, a unique hallmark of $BVMO_{Af1}$. In addition, the oxygenating C4a-(hydro)peroxyflavin intermediate could be spectrophotometrically detected and it was found to be the most stable among all analyzed BVMOs. To assess the possible influence of some residues on the kinetic features, model-inspired site-directed mutagenesis was performed. Among the mutants, the Q436A variant showed a slightly broader substrate scope and a better catalytic efficiency. In summary, this study describes for the first time the kinetic parameters for an eukaryotic BVMO.

1. Introduction

Flavin-dependent monooxygenases are an emerging family of enzymes with valuable potential in biocatalysis due to their ability of performing specific oxidations in a highly selective fashion [1]. Baeyer–Villiger monooxygenases (BVMOs) belong to a subclass of flavoproteins [2]. These enzymes are NADPH dependent and are capable to carry out the so-called Baeyer–Villiger oxidation (the insertion of an oxygen atom in a C–C bond next to a carbonyl group). Interestingly, BVMOs are also able to achieve electrophilic oxidations of heteroatom-containing molecules (i.e. sulfur, nitrogen or boron compounds) and epoxidations [3]. In the last two decades, the research on these oxidative biocatalysts has intensified. Most efforts have been directed to the discovery of new representatives [4] and to the improvement of the already available BVMOs by novel cofactor-regenerating systems [5], site-directed mutagenesis [6] and directed evolution [7].

For a long time, cyclohexanone monooxygenase (CHMO) from *Acinetobacter* sp. NCIB 9871 was the only BVMO studied. The kinetic mechanism of CHMO was first described in the early '80s by the Walsh group [8]. Later, a more detailed study was performed which confirmed the initially proposed mechanism [9]. In the catalytic cycle of CHMO, NADPH rapidly binds to the enzyme and the oxidized flavin is reduced in a fast process by a stereoselective hydride transfer. After this, the reduced flavin reacts with molecular oxygen (O_2) to form the crucial catalytic oxygenating intermediate, the C4a-peroxyflavin. In the absence of substrate the oxygenated flavin intermediate decays slowly, which explains the low activity of CHMO as NADPH oxidase (uncoupling activity). The reaction of the peroxyflavin with a carbonylic substrate is predicted to form the so-called “Criegee adduct”. By an intermolecular rearrangement, the final product is formed and released. It is worth noting that during all the catalytic steps described above, the oxidized coenzyme ($NADP^+$) remains bound to the enzyme. The release of $NADP^+$ completes the catalytic cycle. For CHMO, this is the main rate-limiting step in catalysis. The only other BVMO for which the kinetic mechanism has been elucidated is the thermostable phenylacetone monooxygenase (PAMO) [10]. Also for this bacterial BVMO the release of the oxidized coenzyme, or an associated conformational change in the enzyme structure, limits the

* Corresponding author. Present address: IMIBIO-SL CONICET, Facultad de Química Bioquímica y Farmacia, Universidad Nacional de San Luis, CP 5700 San Luis, Argentina. Tel.: +54 0266 4520300/1623.
E-mail addresses: mlmascotti@unsl.edu.ar, lauramascotti6@hotmail.com (M.L. Mascotti).

http://dx.doi.org/10.1016/j.biochi.2014.09.005
0300-9084/

rate of catalysis. Recently, a preliminary kinetic analysis has been performed on another type of BVMO, FMO-E from *Rhodococcus* sp. RHA1. This again indicated that the rate-limiting step is the slow release of the oxidized coenzyme [11]. Based on these observations, the mechanism originally elucidated for CHMO seems to be valid for all BVMOs.

We have recently identified a BVMO from the fungus *Aspergillus fumigatus* Af293 named $BVMO_{Af1}$ [12] and shown that this enzyme displays some distinctive biochemical features compared to other BVMOs. While all previous kinetic studies on BVMOs have been performed on bacterial representatives, we set out to explore the kinetic properties of this fungal enzyme. In this paper, we report the kinetic mechanism of $BVMO_{Af1}$ and a mutational analysis based on a homology model. This study unveils unique kinetic features of this newly discovered eukaryotic BVMO.

2. Materials and methods

2.1. Materials

All the chemicals and auxiliary enzymes (Phusion DNA polymerase and restriction enzymes) were obtained from Acros Organics, Sigma–Aldrich, Roche Applied Sciences and Fluka. Organic solvents were purchased from Merck and Sintorgan. Oligonucleotide primers were obtained from Sigma. DNA sequencing was conducted at GATC Biotech (Konstanz, Germany).

2.2. Site-directed mutagenesis

For mutagenesis, the previously constructed plasmid pCRE-*BVMO$_{Af1}$* [12] was used as a template. This vector harbors the *BVMO$_{Af1}$* domain (1614 bp; NCBI: XM_742067) fused to the cofactor regenerating enzyme phosphite dehydrogenase (PTDH) [13]. Mutants were constructed using the Quick-Change® site-directed mutagenesis kit from Stratagene following the recommendations of the manufacturer. Primer sequences are shown in the Supplementary information.

2.3. Bacterial cell culture and enzyme purification

Wild type (WT) and single-amino acid variants of 6xHis-tagged $BVMO_{Af1}$ were expressed in *Escherichia coli* TOP10 and purified by affinity chromatography employing a Ni^{2+}-sepharose HP resin (GE Healthcare) and 50 mM Tris/HCl buffer with increasing amounts of imidazole, followed by a desalting step with an Econo-Pac 10DG column (Bio-Rad) pre-equilibrated with the same buffer. Enzyme concentration was determined by measuring the absorbance at λ_{max}, using the extinction coefficient of the WT enzyme $\varepsilon_{449} = 13.3\ mM^{-1}\ cm^{-1}$. Purification from 100 mL culture yielded 1.9 mg of WT ($\varepsilon_{449} = 13.3\ mM^{-1}\ cm^{-1}$), 2.6 mg of Q164H ($\varepsilon_{447} = 16.8\ mM^{-1}\ cm^{-1}$), 3.1 mg of H247A ($\varepsilon_{445} = 15.29\ mM^{-1}\ cm^{-1}$) and 2.0 mg of Q436A ($\varepsilon_{445} = 12.13\ mM^{-1}\ cm^{-1}$). In each case, the ratio $A_{\lambda_{max}}/A_{280}$ was measured to estimate the amount of purified holo enzyme.

2.4. Steady state kinetics

Enzyme activity was measured in a Perkin–Elmer Lambda Bio40 spectrophotometer by monitoring the substrate-dependent decrease in NADPH absorbance at 340 nm ($\varepsilon_{340} = 6.22\ mM^{-1}\ cm^{-1}$). Reaction mixtures contained 50 mM Tris/HCl pH 8.0, 100 μM NADPH, variable concentration of substrate *rac*-bicyclo[3.2.0]hept-2-en-6-one and 0.1–0.8 μM enzyme. All kinetic measurements were performed at 25 °C using air-saturated buffer. The experimental data were fitted to the Michaelis–Menten equation and analyzed by non-linear regression using the SigmaPlot software (SigmaPlot for Windows version 12.0) [14].

The dissociation constant of WT-$BVMO_{Af1}$ for $NADP^+$ was measured by monitoring the change in the flavin-absorbance spectrum upon titration of 50 μM of enzyme with 0–500 μM of $NADP^+$. The decrease in absorbance at 377 nm, induced by $NADP^+$ binding, was used to determine the amount of [E_{ox}–$NADP^+$] and [$NADP^+$]$_{free}$. The K_d was determined by plotting these two concentrations against each other and fitting with the dissociation equation [15] by means of non-linear regression using the SigmaPlot software.

The flavin absorbance during steady state catalysis was determined by measuring the absorbance at 446 nm over time employing an Applied Photophysics SX18MW stopped-flow apparatus. For this, 20 μM $BVMO_{Af1}$ was aerobically mixed with one volume of 200 μM NADPH and 4.0 mM of *rac*-bicyclo[3.2.0]hept-2-en-6-one in 50 mM Tris/HCl pH 8.0. As a reference, the absorbance of the fully oxidized $BVMO_{Af1}$ was set as 100% and the absorbance of the fully reduced enzyme as 0%. All measurements were repeated three times.

2.5. Pre-steady state kinetics

Both the reductive half-reaction of WT-$BVMO_{Af1}$ and the mutants, and the oxidative half-reaction of WT-$BVMO_{Af1}$ were studied by using the stopped-flow technique. All experiments were performed in 50 mM Tris/HCl pH 8.0, at 25 °C. The anaerobic conditions were achieved by flushing the solutions and the system with N_2 and removing the traces of oxygen by adding 10 mM of glucose and a catalytic amount of glucose oxidase in all anaerobic solutions.

Reduction of FAD-bound to $BVMO_{Af1}$ by NADPH was assessed anaerobically at different concentrations of the nicotinamide coenzyme ranging from 20 to 250 μM (final concentrations) at a fixed wavelength (446 nm) recording the absorbance during 0–60 s. In addition, the presence of 2.0 mM of substrate on the kinetics was evaluated. The obtained data were fitted by means of a logarithmic function using the Pro-K software (Applied Photophysics). When the reduction rates of the mutants were studied, 100 μM of NADPH was used. Each reaction condition was measured in triplicate.

The reaction of the reduced enzyme with O_2 was monitored using a photodiode array detector with a spectral scan rate of 2.0 ms. For these experiments, 50 μM $BVMO_{Af1}$ was reduced anaerobically with 80 μM NADPH in the presence of 50 μM $NADP^+$ (to assure binding of $NADP^+$). The reduced $BVMO_{Af1}$ was subsequently mixed with aerated buffer to study the rate of peroxyflavin formation and subsequent decay. In a different experiment, the reduced enzyme was mixed with an equal volume of aerated buffer containing 4.0 mM *rac*-bicyclo[3.2.0]hept-2-en-6-one. 1000 spectra were collected in 1000 s and analyzed by spectral deconvolution by means of non-linear least squares fitting yielding the observed rate constants using the Pro-K software. All measurements were performed in triplicate.

3. Results

3.1. Steady state kinetic analysis

As we previously described, $BVMO_{Af1}$ exhibits a typical Michaelis–Menten kinetic behavior towards aromatic sulfides and some ketones. Intriguingly, the k_{cat} values for all identified substrates are very similar ($k_{cat} \approx 0.5\ s^{-1}$) [12]. In this work, the kinetic parameters of $BVMO_{Af1}$ towards the substrate bicyclo[3.2.0]hept-2-en-6-one were determined (Table 1). Next, the redox state of the flavin cofactor during catalysis was measured in a stopped-flow apparatus in the presence of saturating concentrations of NADPH,

Table 1
Individual kinetic rate constants and dissociation constants describing the catalytic cycle of $BVMO_{Af1}$.

Steady state			
Parameter			Measured value
$k_{cat\text{-}BCH}$ (s^{-1})			0.46 ± 0.02
$k_{cat\text{-}BES}$ (s^{-1})[a]			0.47 ± 0.04
$k_{cat\text{-}PPD}$ (s^{-1})[a]			0.40 ± 0.06
k_{unc} (s^{-1})			0.01 ± 0.002
$K_{M,NADPH}$ (μM)			<5.0
$K_{M,BCH}$ (μM)			119 ± 10
Catalytic efficiency-BCH (mM^{-1} s^{-1})			4.1
A_{449} (%)[b]			63
Pre-steady state			
Reductive half-reaction		Oxidative half-reaction	
$K_{d,NADPH}$ (μM)	<<20	k_{ox} (mM^{-1} s^{-1})	86
k_{red} (s^{-1})	1.24 ± 0.02	$k'_{unc} = k_{O1}$ (s^{-1})	10.8
$K^{+}_{d,NADP}$ (μM)	14.5 ± 4.7	k''_{unc} (s^{-1})	0.0112
		k'''_{unc} (s^{-1})	0.0014
		k_{O2} (s^{-1})	2.81

BCH: bicyclo[3.2.0]hept-2-en-6-one, BES: benzyl(ethyl)sulfide, PPD: 3-phenylpentane-2,4-dione. Standard error values for measurements are shown. For k'_{unc}, k''_{unc}, k'''_{unc} and k_{O2} values (obtained out of three independent experiments) associated errors to the non-linear least squares fitting were lower than 2%.

[a] Values were taken from Mascotti et al. [12].

[b] A_{449} represents the amount of oxidized enzyme during steady state catalysis, expressed as percentage (%).

substrate and oxygen. The enzyme was found to be 63% in the oxidized state during steady state catalysis, suggesting that the kinetic step(s) leading to flavin reduction are slower than those of the oxidative part of the catalytic cycle. Alternatively, a slow release of $NADP^+$ can lead to the presence of more oxidized enzyme during the catalytic cycle.

In the absence of substrate, $BVMO_{Af1}$ consumed NADPH at a 50-fold slower rate (k_{unc}) than in the presence of substrate. During this non-productive form of catalysis (uncoupling reaction), only NADPH and O_2 are consumed, yielding $NADP^+$ and hydrogen peroxide (H_2O_2).

3.2. Pre-steady state reaction kinetics

To understand the atypical steady state kinetics behavior of $BVMO_{Af1}$, regarding the similar k_{cat} values on different substrates, pre-steady state analyses were performed [16].

3.2.1. Reductive half-reaction

To determine the pre-steady state kinetic parameters for the reductive half-reaction (Scheme 1), a stopped-flow apparatus was used. The rate of anaerobic reduction of $BVMO_{Af1}$ was monitored using different NADPH concentrations at 25 °C.

For all measured NADPH concentrations (20–250 μM) a similar rate of flavin reduction was observed: 1.24 s^{-1} (Table 1). This rate is surprisingly low when compared with the other characterized BVMOs namely PAMO (k_{red} = 12 s^{-1}, 25 °C) and CHMO (k_{red} = 22 s^{-1}, 4 °C) [9,10]. The fact that the k_{red} value was independent of the tested NADPH concentrations suggests that the affinity for NADPH is below the minimal coenzyme concentration assessed (20 μM). Besides, no step prior to the flavin reduction could be detected, strongly suggesting that NADPH binding is a fast process and/or has no effect on the flavin absorption spectra. Furthermore, the observed reduction correlates with complete reduction of the flavin cofactor, as evidenced by an almost complete bleaching of the absorbance at 446 nm. This indicates that the flavin reduction is virtually irreversible. This was confirmed by the chemical-reduction of the enzyme with sodium dithionite (data not shown) which resulted in a similar decay in absorbance at 446 nm upon reduction. Interestingly, the rate of NADPH-mediated flavin reduction is only 2.5-fold higher compared to the k_{cat}, confirming that the reduction rate plays a role in setting the limit of the maximal rate of catalysis.

To get insight into the catalytic steps involved in the release of $NADP^+$ the reverse reaction, i.e. the binding of the oxidized coenzyme to the oxidized $BVMO_{Af1}$, was monitored by a titration experiment (Supplementary Fig. S2). The most prominent change in absorbance was observed at 377 nm due to the formation of the E_{ox}—$NADP^+$ complex. Using the $NADP^+$ dependent change in absorbance at 377 nm (ΔA_{377}), the binding constant was determined; $K_{d,NADP^+}$ = 14.5 μM, confirming the tight binding of the oxidized nicotinamide coenzyme. In fact, the determined K_d value only reflects the upper limit of the dissociation constant, due to the presence of PTDH in the system which also binds $NADP^+$. For other BVMOs it has been found that the K_d for the reduced coenzyme is lower when compared with the oxidized coenzyme [9,10]. This is in agreement with the observed low $K_{d,NADPH}$ for $BVMO_{Af1}$.

3.2.2. Oxidative half-reaction

The reactions of reduced $BVMO_{Af1}$ with O_2 were monitored by rapidly mixing reduced $BVMO_{Af1}$ with oxygen-containing buffer. In a first experiment, the reduced $BVMO_{Af1}$ was mixed with oxygenated buffer in order to monitor the uncoupling reaction (Scheme 2). Deconvolution of the spectral scans yielded well-defined spectra for four species, suggesting a three-step process during the oxidative half-reaction (Fig. 1). The formation of the C4a-peroxyflavin, indicated by the formation of a spectrum with an absorbance maximum at 347 nm, was found to be a fast process k'_{unc} = 11.2 s^{-1}. Interestingly, this λ_{max} was found to be somewhat lower when compared with peroxyflavin intermediates reported previously. A subtle change in the C4a-peroxyflavin intermediate spectra was observed with a rate of k''_{unc} = 0.0112 s^{-1}. This spectral change is compatible with the generation of a previously postulated protonated form of the C4a-peroxyflavin; the so-called C4a-(hydro)peroxyflavin [9] while it may also reflect a conformational change. The decay of the latter intermediate into the oxidized flavin was extremely slow, with a rate of 0.0014 s^{-1} (Fig. 1-B). It has been reported that the C4a-(hydro)peroxyflavin intermediate is quite stable for other BVMOs. For example in PAMO the peroxyflavin decays at a rate of 0.01 s^{-1} at 25 °C [10]. However, in the case of $BVMO_{Af1}$ the decay of the peroxyflavin species was found to be remarkably slow, indicating an even higher stability of the $BVMO_{Af1}$-C4a-(hydro)peroxyflavin intermediate.

To determine the oxidation rate in the presence of the substrate, the anaerobically-reduced enzyme was mixed with oxygenated buffer containing the substrate (Scheme 3). Under these conditions, spectral deconvolution yielded three different spectral species, suggesting a two-step process (Fig. 2). The formation of the C4a-peroxyflavin intermediate was again a fast process (k_{O1} = 10.8 s^{-1}) and independent on the presence of substrate, since it is similar when compared with the observed rate in the absence of substrate (*vide supra*). However, in the presence of substrate the

$$E_{ox} + NADPH \underset{}{\overset{K_d}{\rightleftharpoons}} E_{ox}\text{-}NADPH \xrightarrow{k_{red}} E_{red}\text{-}NADP^+$$

Scheme 1. Reduction of $BVMO_{Af1}$ by NADPH.

$$E_{red}\text{-}NADP^+ + O_2 \xrightarrow{k'_{unc}} E_{OO1}\text{-}NADP^+ \xrightarrow{k''_{unc}} E_{OOH2}\text{-}NADP^+ \xrightarrow{k'''_{unc}} E_{ox}\text{-}NADP^+$$

Scheme 2. Oxidative half-reaction in the absence of substrate (uncoupling reaction).

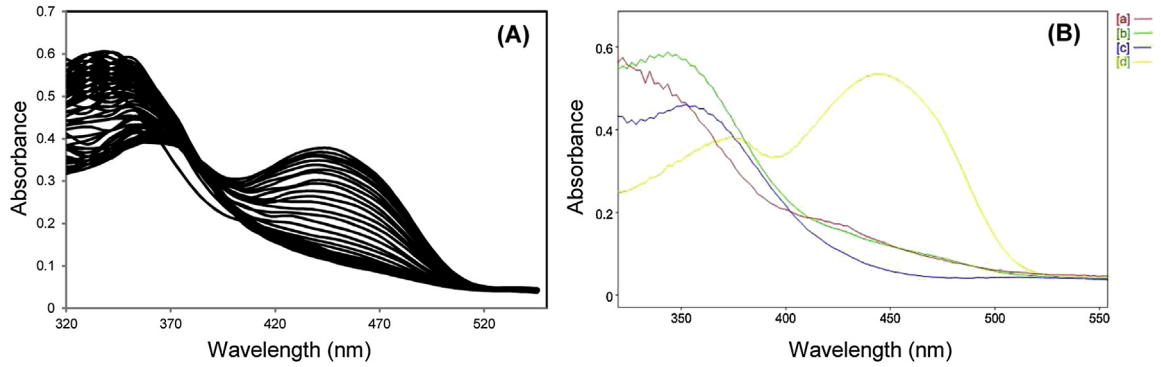

Fig. 1. A) Selected spectra of the reaction of NADPH-reduced $BVMO_{Af1}$ with aerated buffer. B) Spectra of the deconvoluted enzyme species. By means of numerical integration (Pro-K, Applied Photophysics Ltd.), the spectra were fitted using a three-step kinetic model (A→B→C→D). The first step corresponds to the formation of the C4-peroxyflavin intermediate (E_{OO1}-$NADP^+$), the second step presumably represents the formation of the C4-(hydro)peroxyflavin (E_{OOH2}-$NADP^+$) species and the third step corresponds to the decay of the intermediate to the species E_{ox}-$NADP^+$.

$$E_{red}\text{-}NADP^+ + O_2 \xrightarrow{k_{O1}} E_{OO}\text{-}NADP^+ + \text{Substrate} \xrightarrow{k_{O2}} E_{ox}\text{-}NADP^+ + \text{Product}$$

Scheme 3. Oxidative half-reaction in the presence of substrate.

formation of the (presumed) protonated peroxyflavin species was not observed, probably because of the rapid reaction with the substrate to undergo a Baeyer–Villiger oxidation while regenerating the oxidized flavin cofactor. The reaction with the substrate proceeded with a rate of $k_{O2} = 2.8\ s^{-1}$. Finally, a subtle spectral change was observed with a rate of $0.16\ s^{-1}$, which may be due to a conformational change or release of $NADP^+$ (species C→D, Fig. 2-B).

As it has been previously demonstrated for other BVMOs the rate of formation of the C4a-peroxyflavin increases linearly with O_2 concentration. The second order rate constant (k_{ox}) for the generation of the C4a-peroxyflavin intermediate was found to be $86\ mM^{-1}\ s^{-1}$. Fully aerated buffer (0.25 mM O_2) would give a rate of $21.6\ s^{-1}$, which is ~40-fold faster than the k_{cat}. This indicates that during steady state catalysis the oxygenation of the reduced enzyme to form the peroxyflavin enzyme intermediate is not a rate-limiting step. The subsequent step observed during the oxidative half-reaction proceeds slowly ($k_{O1} > k_{O2}$). This value lumps the sequential steps of substrate's entry into the catalytic pocket, reaction of the substrate with the peroxyflavin, formation of the Criegee adduct, and release of the product with the concomitant re-oxidation of the flavin cofactor. For other BVMOs, a kinetic event after the Baeyer–Villiger oxidation has been described as the rate-limiting step. In CHMO, it has been identified as the release of $NADP^+$ while for PAMO it has been proposed a conformational change previous to the release of the oxidized coenzyme. For $BVMO_{Af1}$ we did not observe a spectral change that could be linked with $NADP^+$ release. However, this process could contribute to the relatively low k_{cat} of the fungal enzyme, while the rate of reduction and the Baeyer–Villiger oxidation mainly limit the rate of catalysis.

3.3. Comparative analyses of a $BVMO_{Af1}$ model structure

To probe the catalytic role of specific residues in $BVMO_{Af1}$, single amino acid substitutions were proposed based on a structural homology model of this eukaryotic enzyme. A $BVMO_{Af1}$ model was constructed [17] by using as template the crystal structure of PAMO (PBD entry 2YLT.A) [18] displaying 41.8% sequence identity with $BVMO_{Af1}$ (Supplementary Fig. S3).

As in the case of PAMO, $BVMO_{Af1}$ is predicted to have two domains, the FAD binding domain (1–148, 380–511) and the NADPH binding domain (149–379). The crucial catalytic Arg residue [19] (R337 in PAMO, R329 in $BVMO_{Af1}$) and the Asp residue [20] that gives the proper positioning of NADPH in the active site (D66 in PAMO, D54 in $BVMO_{Af1}$), are conserved (asterisks in Supplementary Fig. S3). As we have previously described, $BVMO_{Af1}$ has a single non-conservative amino acid change in the BVMO-identifying fingerprint motif (Supplementary Fig. S4) [12]. The respective His residue is replaced by Gln. The role of this central histidine has been

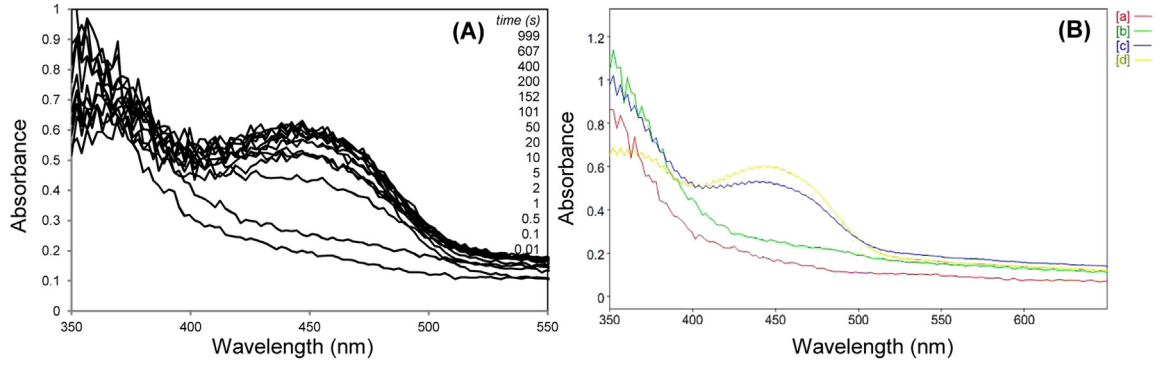

Fig. 2. A) Selected spectra of the reaction of NADPH-reduced $BVMO_{Af1}$ with aerated buffer containing 2.0 mM of bicyclo[3.2.0]hept-2-en-6-one (final concentration in the cell). The presented spectra were recorded at the indicated times. B) Spectra of the deconvoluted enzyme species. By means of numerical integration, the spectra were derived using a two-step kinetic model (A→B→C). The first step corresponds to the oxygenation of the reduced enzyme (E_{red}-$NADP^+$ → E_{OO}-$NADP^+$) and the second step represents the substrate-dependent re-oxidation of the enzyme (E_{OO}-$NADP^+$ → E_{ox}-$NADP^+$). A third step was also evidenced which presumably corresponds to a conformational change (C→D).

proposed to facilitate the conformational changes during a catalytic cycle. It has been also reported that replacing this residue with an alanine inactivates 4-hydroxyacetophenone monooxygenase (HAPMO) by preventing FAD binding [21], and significantly reduces the catalytic efficiency of CHMO by diminishing its affinity for NADPH [22]. Therefore, it was hypothesized that by substituting Q164 by His in $BVMO_{Af1}$ the catalytic efficiency would be improved. Another target residue was H247 in the NADPH binding domain of $BVMO_{Af1}$. In PAMO and other BVMOs, glycine or alanine residues are found at the analogous position. Inspection of the structures reveals that this residue is near the active site and in proximity of the cofactor and the coenzyme. We hypothesized that the relatively bulky H247 may negatively affect the rate of catalysis.

Finally, in the FAD binding site $BVMO_{Af1}$ bears a substitution of the consensus Met (M446 in PAMO) by a Gln (Q436 in $BVMO_{Af1}$). It has been reported that the active site of PAMO widens and changes its shape when M446 is replaced by a smaller amino acid [7c], resulting in largely altered substrate acceptance profiles and enantioselectivities. We hypothesize that Q436 may reduce the substrate specificity of $BVMO_{Af1}$ by steric hindrance and may also affect the hydride transfer from NADPH to FAD, thus decreasing the reduction rate.

Based on the above mentioned, the single amino acids variants of $BVMO_{Af1}$ Q164H, H247A and Q436A were constructed expressed and characterized.

3.4. Characterization of single amino acid $BVMO_{Af1}$ variants

3.4.1. Spectral properties

The three variants exhibited typical flavin-absorbance spectra and were able to oxidize NADPH. These results demonstrate that the proposed single amino acid changes did not affect the FAD binding nor the coenzyme binding capacity, indicating that the overall folding of these proteins was correct (Supplementary Fig. S5). Surprisingly, despite the modification of residues highly conserved among BVMOs, no drastic effects other than changes in the extinction coefficients were observed for any of these variants.

3.4.2. Steady state kinetics

To evaluate the effect of these mutations on the rate of catalysis, steady state kinetic measurements were carried out (Table 2). The single amino acid replacements Q164H and H247A showed no effect on the catalytic efficiency of the enzyme. A subtle change was observed in the Q436 variant, where the catalytic efficiency increased 2-fold. This mainly reflected a change in apparent substrate affinity, since a 3-fold reduction of the K_M value was observed. While this is a small change, it suggests a role of this residue in forming the substrate binding pocket or in positioning the FAD facing the substrate.

3.4.3. Rapid reaction kinetics: reductive half-reaction

In order to evaluate the effect of these single-amino acid substitutions on the rate-limiting step, the reductive half-reaction was studied by using the stopped-flow technique (Table 2). The obtained k_{red} values revealed that in general these mutations do not significantly affect the apparent reduction rate. However, in the mutant Q436A the reduction rate seems to proceed 2-times faster ($k_{red} = 2.55\ s^{-1}$) compared to the wild type enzyme.

Table 2
Steady state and pre-steady state kinetic parameters of $BVMO_{Af1}$ mutants towards *rac*-bicyclo[3.2.0]hept-2-en-6-one.

Variant	Steady state			Pre-steady state
	K_M (μM)	k_{cat} (s^{-1})	k_{cat}/K_M ($mM^{-1}\ s^{-1}$)	k_{red} (s^{-1})
Q164H	101 ± 23	0.38 ± 0.02	3.75	1.57
H247A	104 ± 16	0.31 ± 0.01	3.0	1.39
Q436A	43 ± 13	0.26 ± 0.02	6.04	2.55

4. Discussion

Although it has been stated that fungal genomes are rich in BVMO-encoding genes [23], very few fungal recombinant BVMOs have been available for study. The first eukaryotic BVMO cloned and biocatalytically characterized was the cycloalkanone monooxygenase (CAMO) from *Cylindrocarpon radicicola* [24]. It was shown that this enzyme resembles the well-known CHMO concerning its substrate specificity. Recently, we have described the first Aspergilli belonging BVMO, $BVMO_{Af1}$, from *A. fumigatus* Af293. We characterized this enzyme and discovered that besides typical BVMO hallmarks $BVMO_{Af1}$ shows distinctive features such as its steady state kinetic parameters, the restricted substrate specificity and its good stability in different conditions [12]. Regarding the substrate specificity of $BVMO_{Af1}$, it was demonstrated that there are not many accepted molecules as well as no common features among them. Additionally, it was demonstrated that *A. fumigatus* has several BVMO-encoding ORFs, which suggests that these enzymes may have specific roles such as synthesis of defense compounds, secondary metabolism reactions and detoxification mechanisms [25]. All these features make it interesting to further analyze $BVMO_{Af1}$ from a mechanistic perspective, to understand the atypical catalytic behavior of $BVMO_{Af1}$, mainly evidenced by its substrate-independent k_{cat} values.

For this eukaryotic enzyme the catalytic cycle starts when fully oxidized $BVMO_{Af1}$ is reduced by the coenzyme NADPH. Surprisingly, we found that this step (k_{red}) is relatively slow ($1.24\ s^{-1}$), which is an unexpected fact since usually BVMOs are efficient in using NADPH as an electron donor [26]. After this step, $BVMO_{Af1}$ reacts with O_2 to form the crucial catalytic enzyme intermediate C4a-(hydro)peroxyflavin. In the absence of a suitable substrate, this intermediate was found to be remarkably stable in $BVMO_{Af1}$. In the presence of a suitable substrate, such as bicyclo[3.2.0]hept-2-en-6-one, the peroxyflavin intermediate is also rapidly formed ($k_{ox} = 86\ mM^{-1}\ s^{-1}$) and subsequently reacts with the substrate. Finally, the oxidation product is formed and the enzyme releases the oxidized nicotinamide coenzyme to start a new catalytic cycle. The overall kinetic mechanism of $BVMO_{Af1}$ is presented in Fig. 3. For the already characterized bacterial BVMOs, it has been described that kinetic steps after oxygenating the substrate limit the rate of catalysis, meaning a conformational change and/or release of $NADP^+$. Strikingly, in the case of $BVMO_{Af1}$, a major contribution to the overall catalytic rate was found to be the k_{red}, while also the substrate oxidation and possibly the release of $NADP^+$ contribute to the k_{cat}. Such a relatively slow rate of flavin reduction has not been observed before for other BVMOs.

In view of these findings, we hypothesize that $BVMO_{Af1}$ might be a physiologically efficient enzyme, since it does not lead to wasteful consumption of NADPH. Also, the high stability of the C4a-(hydro)peroxyflavin intermediate can be considered as a cellular mechanism to avoid the release of high amounts of toxic hydrogen peroxide in the absence of a suitable substrate. Recently, it has been reported that deepoxy-synerazol accumulates in an *A. fumigatus* Af293 strain lacking *$BVMO_{Af1}$* gene (Δ*psoE*), supporting the monooxygenase activity of this enzyme *in vivo* [27]. In addition this supports our previous statement that the physiological substrate of $BVMO_{Af1}$ is remarkably different from the reference compounds usually employed to detect Baeyer–Villiger activity.

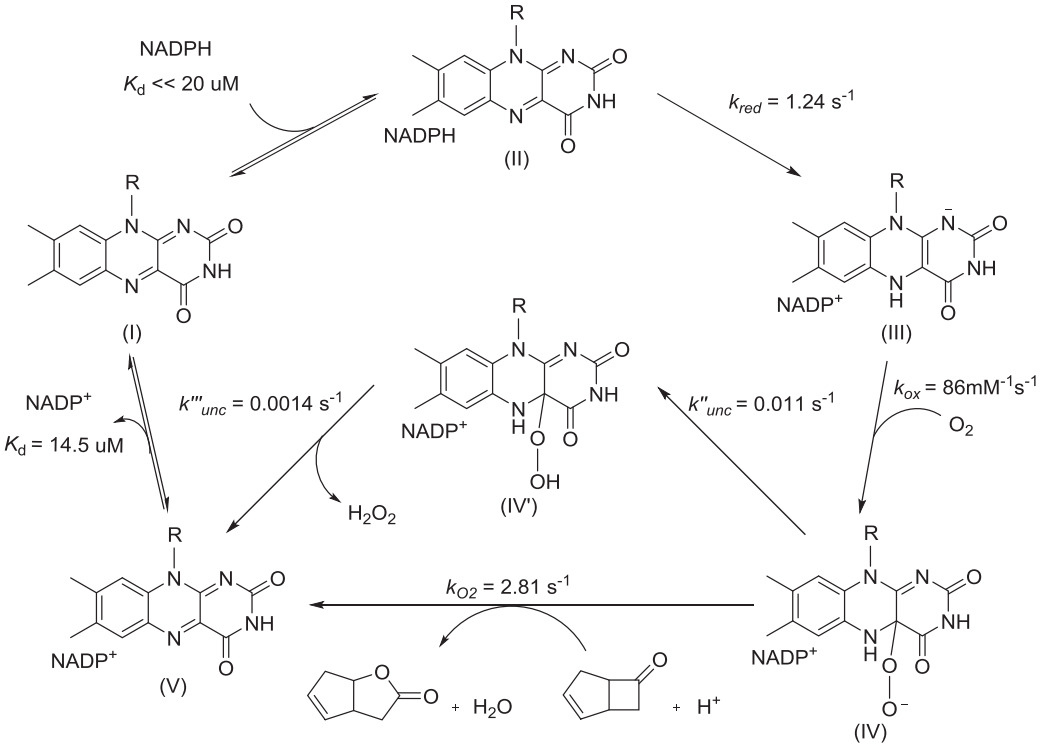

Fig. 3. Proposed catalytic cycle for $BVMO_{Af1}$. Numbers indicate the observed flavin intermediates. The catalytic cycle starts with oxidized $BVMO_{Af1}$ (I), which after binding of NADPH (II) is reduced (III). Reduced $BVMO_{Af1}$ reacts with O_2, yielding the intermediate C4a-peroxyflavin (IV). In the absence of substrate the intermediate transforms to a second species, probably the C4a-(hydro)peroxyflavin (IV′), that lastly decays to the oxidized $BVMO_{Af1}$ complexed with $NADP^+$ (V). In the presence of substrate, the C4a-peroxyflavin intermediate reacts to produce the Baeyer–Villiger product and the oxidized enzyme remains bound to $NADP^+$ (V). Finally the oxidized enzyme releases the oxidized coenzyme to be available to start a new cycle. The individual rate constants and binding affinities appear above/next to the arrows.

With the aim of getting insight into the kinetic features of $BVMO_{Af1}$, a structure-guided enzyme engineering study was performed. Unfortunately, up to date crystallization experiments have not been successful for $BVMO_{Af1}$. For this reason, a homology model of $BVMO_{Af1}$ was constructed. Based on the structural model, three $BVMO_{Af1}$ mutants were generated. Characterization of these mutant enzymes revealed that only one amino acid replacement had effects on the kinetic properties: the Q436A mutant displayed a lower K_M value for the substrate and an increased rate of NADPH-mediated flavin reduction. This supports the initial proposition that this residue is part of the active site. These results show that although the residues selected for mutagenesis are highly conserved among BVMOs, in $BVMO_{Af1}$ their substitution does not significantly affect catalysis. It also demonstrates that in this fungal enzyme a more complex set of factors govern its rate of catalysis as well as its substrate specificity.

5. Conclusions

This study reveals unique features in the kinetic mechanism of the fungal enzyme $BVMO_{Af1}$. It was demonstrated that the catalytic rate is partly limited by the hydride transfer from NADPH to the flavin (reduction rate). Moreover, it was determined that the peroxyflavin intermediate is extremely stable. Finally, by structure-inspired mutations it was confirmed that the Q436 residue plays a role in catalysis by $BVMO_{Af1}$. All these new insights, along with the presence of numerous BVMOs encoding genes in fungi, highlight the importance of characterizing new eukaryotic members of this family.

Conflict of interest

None declared.

Acknowledgments

Erasmus Mundus External Action 2 Programme is acknowledged for the financial support granted to MLM. This work was supported by grants from UNSL-PROICO 2-1412, ANPCyT-PICT 2011-1416 and CONICET-PIP 2012-2014-00360 to MKS and PICT 2010-1468 to MJA. MLM is a postdoctoral CONICET fellow. MJA and MKS are members of the CONICET Research Career. MWF was supported by the EU-FP7 Oxygreen project 212281. We also thank to two anonymous reviewers for their helpful criticisms and suggestions.

Appendix A. Supplementary data

Supplementary data related to this article can be found at http://dx.doi.org/10.1016/j.biochi.2014.09.005.

References

[1] a) V. Joosten, W.J.H. van Berkel, Flavoenzymes, Curr. Opin. Chem. Biol. 11 (2007) 195–202;
b) D.E. Torres Pazmiño, M. Winkler, A. Glieder, M.W. Fraaije, Monooxygenases as biocatalysts: classification, mechanistic aspects and biotechnological applications, J. Biotechnol. 146 (2010) 9–24.
[2] a) D.E. Torres Pazmiño, H.M. Dudek, M.W. Fraaije, Baeyer-Villiger monooxygenases: recent advances and future challenges, Curr. Opin. Chem. Biol. 14 (2009) 1–7;
b) H. Leisch, K. Morley, P.C.K. Lau, Baeyer-Villiger monooxygenases: more than just green chemistry, Chem. Rev. 111 (2011) 4165–4222.
[3] a) G. de Gonzalo, D.E. Torres Pazmiño, G. Ottolina, M.W. Fraaije, G. Carrea, Oxidations catalyzed by phenylacetone monooxygenase from *Thermobifida fusca*, Tet. Asymm. 16 (2005) 3077–3083;
b) G. de Gonzalo, M.D. Mihovilovic, M.W. Fraaije, Recent developments in the application of Baeyer-Villiger monooxygenases as biocatalysts, ChemBioChem 11 (2010) 2208–2231.

[4] a) M. Kadow, S. Saß, M. Schmidt, U.T. Bornscheuer, Recombinant expression and purification of the 2,5-diketocamphane 1,2-monooxygenase from the camphor metabolizing *Pseudomonas putida* strain NCIMB 10007, AMB Express 1 (2011) 13;
b) A. Riebel, H.M. Dudek, G. de Gonzalo, P. Stepniak, L. Rychlewski, M.W. Fraaije, Expanding the set of rhodococcal Baeyer-Villiger monooxygenases by high-throughput cloning, expression and substrate screening, Appl. Microbiol. Biotechnol. 95 (2012) 1479–1489;
c) H. Leisch, R. Shi, S. Grosse, K. Morley, H. Bergeron, M. Cygler, H. Iwaki, Y. Hasegawa, P.C.K. Lau, Cloning, Baeyer-Villiger biooxidations, and structures of the camphor pathway 2-oxo-3-4,5,5-trimethylcyclopentenylacetyl-coenzyme A monooxygenase of *Pseudomonas putida* ATCC 17453, Appl. Environ. Microbiol. 78 (2012) 2200–2212.

[5] a) F. Hollmann, A. Taglieber, F. Schulz, M.T. Reetz, A light-driven stereoselective biocatalytic oxidation, Angew. Chem. Int. Ed. 16 (2007) 1–5;
b) W.H. Lee, J.B. Park, K. Park, M.D. Kim, J.H. Seo, Enhanced production of ε-caprolactone by overexpression of NADPH-regenerating glucose 6-phosphate dehydrogenase in recombinant *Escherichia coli* harboring cyclohexanone monooxygenase gene, Appl. Microbiol. Biotechnol. 76 (2007) 329–338;
c) S. Staudt, U.T. Bornscheuer, U. Menyesc, W. Hummeld, H. Gröger, Direct biocatalytic one-pot-transformation of cyclohexanol with molecular oxygen into ε-caprolactone, Enzyme Microb. Technol. 53 (2013) 288–292.

[6] a) C.M. Clouthier, M.K. Kayser, Increasing the enantioselectivity of cyclopentanone monooxygenase (CPMO): profile of new CPMO mutants, Tet. Asymm. 17 (2006) 2649–2653;
b) M.T. Reetz, S. Wu, Laboratory evolution of robust and enantioselective Baeyer-Villiger monooxygenases for asymmetric catalysis, J. Am. Chem. Soc. 131 (2009) 15424–15432;
c) D.E. Torres Pazmiño, R. Snajdrova, D.V. Rial, M.D. Mihovilovic, M.W. Fraaije, Altering the substrate specificity and enantioselectivity of phenylacetone monooxygenase by structure-inspired enzyme redesign, Adv. Synth. Catal. 348 (2007) 1361–1368.

[7] a) A. Kirschner, U.T. Bornscheuer, Directed evolution of a Baeyer-Villiger monooxygenase to enhance enantioselectivity, Appl. Microbiol. Biotechnol. 81 (2008) 465–472;
b) Z.G. Zhang, G.D. Roiban, J.P. Acevedo, I. Polyak, M.T. Reetz, A new type of stereoselectivity in Baeyer-Villiger reactions: access to E- and Z-olefins, Adv. Synth. Catal. 355 (2013) 99–106;
c) H.M. Dudek, M.J. Fink, A.V. Shivange, A. Dennig, M.D. Mihovilovic, U. Schwaneberg, M.W. Fraaije, Extending the substrate scope of a Baeyer-Villiger monooxygenase by multiple-site mutagenesis, Appl. Microbiol. Biotechnol. (2013), http://dx.doi.org/10.1007/s00253-013-5364-1.

[8] C. Cummings Ryerson, D.P. Ballou, C. Walsh, Mechanistic studies on cyclohexanone oxygenase, Biochemistry 21 (1982) 2644–2655.

[9] D. Sheng, D.P. Ballou, V. Massey, Mechanistic studies of cyclohexanone monooxygenase: chemical properties of intermediates involved in catalysis, Biochemistry 40 (2001) 11156–11167.

[10] D.E. Torres Pazmiño, B.J. Baas, D.B. Janssen, M.W. Fraaije, Kinetic mechanism of phenylacetone monooxygenase from *Thermobifida fusca*, Biochemistry 47 (2008) 4082–4093.

[11] A. Riebel, M.J. Fink, M.D. Mihovilovic, M.W. Fraaije, Type II flavin-containing monooxygenases: a new class of biocatalysts that harbors Baeyer-Villiger monooxygenases with a relaxed coenzyme specificity, ChemCatChem (2013), http://dx.doi.org/10.1002/cctc.201300550.

[12] M.L. Mascotti, M. Juri Ayub, H.M. Dudek, M. Kurina Sanz, M.W. Fraaije, Cloning, overexpression and biocatalytic exploration of a novel Baeyer-Villiger monooxygenase from *Aspergillus fumigatus* Af293, AMB Express 3 (2013) 1–10.

[13] D.E. Torres Pazmiño, A. Riebel, J. De Lange, F. Rudroff, M.D. Mihovilovic, M.W. Fraaije, Efficient biooxidations catalyzed by a new generation of self-sufficient Baeyer–Villiger monooxygenases, ChemBioChem 10 (2009) 2595–2598.

[14] T. Ozaki, S. Mishima, M. Nishiyama, T. Kuzuyama, NovQ is a prenyltransferase capable of catalyzing the addition of a dimethylallyl group to both phenylpropanoids and flavonoids, J. Antibiot. 62 (2009) 385–392.

[15] P. Thordarson, Determining association constants from titration experiments in supramolecular chemistry, Chem. Soc. Rev. 40 (2011) 1305–1323.

[16] N.B. Beaty, D.P. Ballou, The reductive half-reaction of liver microsomal FAD-containing monooxygenase, J. Biol. Chem. 256 (1981) 4611–4618.

[17] CPHmodels 3.2 Server. Available from: www.cbs.dtu.dk/services/CPHmodels.

[18] E. Malito, A. Alfieri, M.W. Fraaije, A. Mattevi, Crystal structure of a Baeyer-Villiger monooxygenase, Proc. Natl. Acad. Sci. USA 101 (2004) 13157–13162.

[19] N.M. Kamerbeek, M.W. Fraaije, D.B. Janssen, Identifying determinants of NADPH specificity in Baeyer-Villiger monooxygenases, Eur. J. Biochem. 271 (2004) 2107–2116.

[20] R. Orru, H.M. Dudek, C. Martinoli, D.E. Torres Pazmiño, A. Royant, M. Weik, M.W. Fraaije, A. Mattevi, Snapshots of enzymatic Baeyer-Villiger catalysis. Oxygen activation and intermediate stabilization, J. Biol. Chem. 286 (2011) 29284–29291.

[21] M.W. Fraaije, N.M. Kamerbeek, W.J.H. van Berkel, D.B. Janssen, Identification of a Baeyer-Villiger monooxygenase sequence motif, FEBS Lett. 518 (2002) 43–47.

[22] M.J. Cheesman, M.B. Kneller, A.B. Rettie, Critical role of histidine residues in cyclohexanone monooxygenase expression, cofactor binding and catalysis, Chem. Biol. Interact. 146 (2003) 157–164.

[23] D.E. Torres Pazmiño, M.W. Fraaije, Discovery, redesign and applications of Baeyer-Villiger monooxygenases, in: M. Tomoko (Ed.), Future Directions in Biocatalysis, Elsevier BV, New York, USA, 2007, pp. 107–127.

[24] F. Leipold, R. Wardernga, U.T. Bornscheuer, Cloning, expression and characterization of a eukaryotic cycloalkanone monooxygenase from *Cylindrocarpon radicicola* ATCC 11011, Appl. Microbiol. Biotechnol. 94 (2011) 705–712.

[25] a) T. Itoh, K. Tokunaga, Y. Matsuda, I. Fujii, I. Abe, Y. Ebizuka, T. Kushiro, Reconstitution of a fungal meroterpenoid biosynthesis reveals the involvement of a novel family of terpene cyclases, Nat. Chem. 2 (2010) 858–864;
b) D. Boettger, C. Hertweck, Molecular diversity sculpted by fungal PKS–NRPS hybrids, ChemBioChem 14 (2013) 28–42.

[26] P. Chaiyen, M.W. Fraaije, A. Mattevi, The enigmatic reaction of flavins with oxygen, Trends Biochem. Sci. 37 (2012) 373–380.

[27] P. Wiemann, C.J. Guob, J.M. Palmer, R. Sekonyelac, C.C.C. Wang, N.P. Keller, Prototype of an intertwined secondary-metabolite supercluster, Proc. Natl. Acad. Sci. USA 110 (2013) 17065–17070.